

Patch Is Not All You Need

Changzhen Li^{1,2,3}, Jie Zhang^{1,2}, Yang Wei, Zhilong Ji⁴, Jinfeng Bai⁴, Shiguang Shan^{1,2,3},

¹Key Lab of Intelligent Information Processing of Chinese Academy of Sciences, Institute of Computing Technology

²University of Chinese Academy of Sciences

³Hangzhou Institute for Advanced Study, UCAS, school of Intelligent Science and Technology

⁴Tomorrow Advancing Life

Abstract

Vision Transformers have achieved great success in computer visions, delivering exceptional performance across various tasks. However, their inherent reliance on sequential input enforces the manual partitioning of images into patch sequences, which disrupts the image’s inherent structural and semantic continuity. To handle this, we propose a novel Pattern Transformer (Patternformer) to adaptively convert images to pattern sequences for Transformer input. Specifically, we employ the Convolutional Neural Network to extract various patterns from the input image, with each channel representing a unique pattern that is fed into the succeeding Transformer as a visual token. By enabling the network to optimize these patterns, each pattern concentrates on its local region of interest, thereby preserving its intrinsic structural and semantic information. Only employing the vanilla ResNet and Transformer, we have accomplished state-of-the-art performance on CIFAR-10 and CIFAR-100, and have achieved competitive results on ImageNet.

1 Introduction

In natural language processing, each word represents a unique concept, and sentences are composed from sequences of these abstract words. Transformer model, by treating each word as a token, leverages the self-attention mechanism to model global contextual relationships, providing a fundamental advantage in processing textual sequences (Vaswani et al. 2017; Devlin et al. 2018; Brown et al. 2020). Inspired by this, Vision Transformer splits images into sequences of patches during the preprocessing phase, which are then treated as visual “words” and fed into the Transformer network (Dosovitskiy et al. 2020). However, despite the significant success of Transformers in vision tasks, the tokenization procedure introduces several challenges: (1) Collapse the structural and semantic information. Unlike natural language where each word constitutes an independent entity adhering to a relatively fixed sentence structure (e.g., Subject + Verb + Object), the structural information in an image is complex and irregular. The manual division disrupts the innate structure of objects within the image, and meanwhile, the image’s variance (e.g., scale, rotation) results in inconsistent semantic sequences for identical objects. (2) Images inherently possess a high degree of redundancy compared to the concise concepts of text. The procedure of manually partitioning images produces a fixed num-

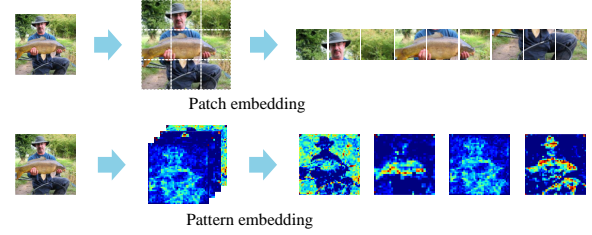


Figure 1: Patches are local spatial features, while Patterns are global semantic features.

ber of patches, many of which are redundant and uninformative for the target class. These redundant patches are not only fail to contribute beneficially but also impose a computational burden on expensive Transformer.

Despite the inherent challenges involved in converting images to sequences, this critical issue has yet to find an effective solution, with most methods persisting with the patchification following ViT (Dosovitskiy et al. 2020). A cohort of researchers have sought to improve the patch embedding methodology. For example, CeiT (Yuan et al. 2021) substitutes the initial linear projection with a convolutional stem, thereby combining the strengths of CNNs in extracting local features. DPT introduces Deformable Patch to adaptively divide patches based on varying positions and scales. TokenLearner (Ryoo et al. 2021) focuses on learning eight crucial visual tokens to model images or videos, however, these tokens, once subjected to global pooling, completely discard spatial information. Another faction strives to mitigate the negative impact of patchification. FlexiViT (Beyer et al. 2023) recognizes the limitation of a fixed patch size and utilizes flexible patch size to design trade-off models. Some suggest removing random (as in MAE (He et al. 2022)) or unimportant (as in A-vit (Yin et al. 2022)) tokens. Although these methods improve the process of converting images to sequences and tackle the issue of the fixed patch size and redundant patches, they still fail to preserve the structural and semantic information within image objects as long as the patch partitioning remains in use.

To address these issues, we propose a novel Pattern Transformer (Patternformer) to adaptively converting images to pattern sequences. These sequences serve as the inputs of Transformer, thereby eliminating complications introduced

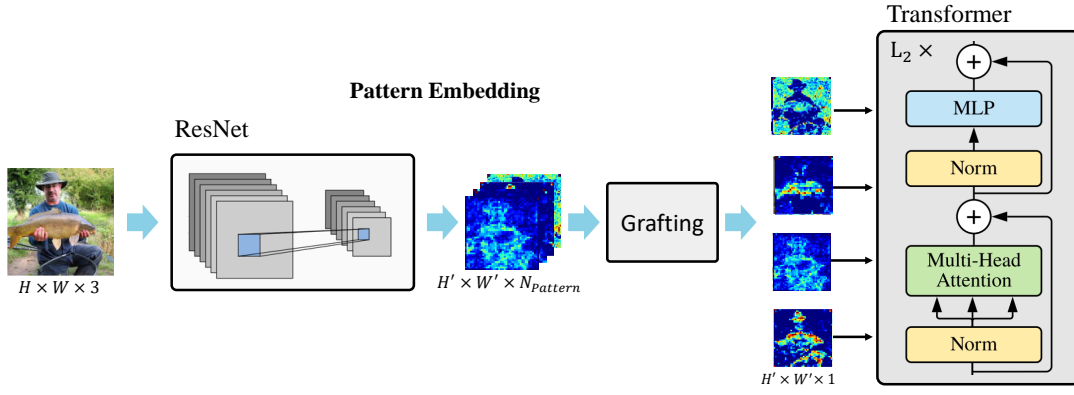


Figure 2: Pipeline. First, capture local semantic patterns by employing the vanilla ResNet, and then model the global context by employing the vanilla ViT, which leverages the strengths of both CNNs and ViTs.

by manual patchification. A pattern typically denotes a specific structure or an underlying rule within an image, such as faces, buildings, vehicles, or parts of some objects. The interpretability of neural networks reveals that certain channels within specific layers capture distinct patterns of local regions (Bau et al. 2017). Based on this, we leverage a convolutional neural network to extract various patterns from the image, with each channel representing a pattern that is fed into the Transformer as a visual token. Converting images into sequences by patterns eliminates the need to manually divide the image into rigid patches based on experiential knowledge. It captures the local region of interest in accordance with network optimization, thus preserving its structural and semantic information. Moreover, the process of pattern embedding does not involve image size and patch size, resulting in a flexible and variable sequence length. This flexibility improves the efficiency of the Transformer’s modeling capabilities.

Overall, we employ CNNs to adeptly capture local patterns and Transformer to model the global context, thus effectively capitalizing on the inherent advantages of both CNNs and Transformer. We conducted extensive experiments and accomplished state-of-the-art performance on CIFAR-10 and CIFAR-100, and achieved competitive results on ImageNet.

2 Related Work

Convolutional Neural Networks Convolutional Neural Networks (CNNs) have emerged as a dominant paradigm in image classification for the last decade. Pioneering architectures such as AlexNet, VGGNet, Inception, ResNet, DenseNet continued to push the boundaries of image classification accuracy through deeper and wider structures (Krizhevsky, Sutskever, and Hinton 2012; Simonyan and Zisserman 2014; Szegedy et al. 2015; He et al. 2016; Huang et al. 2017). Subsequent models like MobileNet, ShuffleNet, EfficientNet, and RegNet focused on a better trade-off of accuracy and efficiency (Howard et al. 2017; Tan and Le 2019; Radosavovic et al. 2020). Despite their success, CNNs inherently struggle to capture long-range dependencies, a capability that can be crucial for comprehending complex scenes.

Vision Transformers Vision Transformers have recently emerged as a promising alternative to CNNs, inspired by the success of Transformers in Natural Language Processing (NLP). ViT (Dosovitskiy et al. 2020) was the first to apply a pure transformer to the sequences of image patches for image classification. Following this, numerous strategies have been proposed to further improve vision transformer. e.g., data efficient (DeiT) (Touvron et al. 2021), modeling local feature (Swin Transformers, TNT, Shuffle Transformer, RegionViT) (Liu et al. 2021; Han et al. 2021; Huang et al. 2021; Chen, Panda, and Fan 2021), improving self-attention layer (DeepViT, KVT, XCiT) (Zhou et al. 2021; Wang et al. 2022; Ali et al. 2021), pyramid architecture (PVT, PiT) (Wang et al. 2021; Heo et al. 2021), Neural architecture search (ViTAS) (Su et al. 2022). However, Vision Transformers require massive training data, and lack the ability to keep the innate structure of objects under various transformations like scale and rotation.

Hybrid Vision Transformers To combine the strengths of both CNNs and ViTs, Hybrid Vision Transformers have been proposed. CvT (Wu et al. 2021), CMT (Guo et al. 2022), CeiT (Yuan et al. 2021), and LocalViT (Li et al. 2021) all bring convolutions into transformers blocks to promote the correlation among neighboring tokens. LeViT (Graham et al. 2021) and BoTNet (Srinivas et al. 2021) resort to a different technology roadmap, replacing former transformers with convolutions, thereby proposing a hybrid neural network for faster inference.

Our Pattern Transformer is also a hybrid Vision Transformers, but we regard each pattern as visual tokens to feed into the Transformer, which is totally different from existing vision transformers.

3 Method

We illustrate the overall diagram of the Pattern Transformer architecture in Figure 2, comprising two primary components. First, capture local semantic patterns by employing the vanilla ResNet (He et al. 2016), and then model the global context by employing the vanilla ViT (Dosovitskiy et al. 2020), which leverages the combined strengths of both CNNs and ViTs.

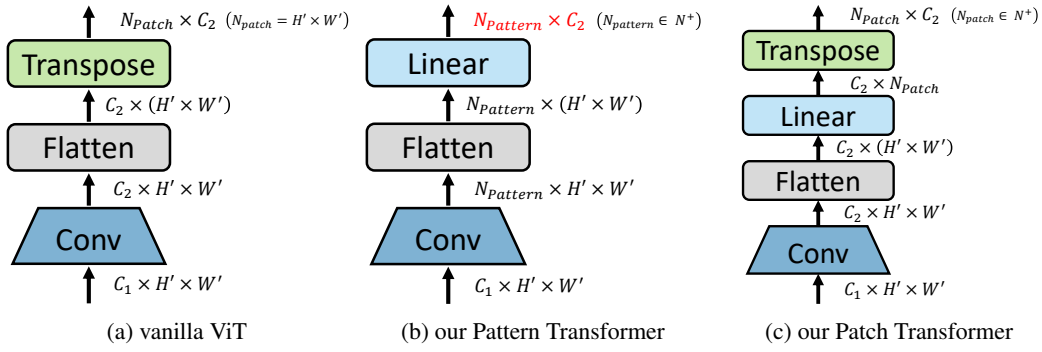


Figure 3: The Grafting combines the ResNet and ViT

Revisiting Vision Transformer The standard Transformer processes a 1D sequence of patch embeddings as input. To accommodate 2D images, ViT reshapes the image $x \in R^{H \times W \times 3}$ into a sequence of flattened 2D patches $x_{patch} \in R^{N_{patch} \times (P^2 \cdot C)}$, where (H, W) represents the resolution of the original image, C represents the number of channels, (P, P) denotes the resolution of each image patch, and $N_{patch} = HW/P^2$ is the resulting number of patches, which also serves as the effective input sequence length for the Transformer. In practice, ViT splits each image into patches with fixed size and positions by employing single or multiple convolution layers, and these patches possess a feature size $1 \times 1 \times C$ and a receptive field $P \times P$. However, this process introduces two limitations: (1) The patch with a $P \times P$ receptive field is hard to be an independent entity, which collapses the structural and semantic information of the original image. (2) The sequence length N is constrained by the values of the image resolution (H, W) and patch size P , and moreover, all N patches are treated equally, even those lacking sufficient discriminative information.

Pattern Embedding Our intuition is that an image can be summarized by a sequence of visual “words”. This contrasts convolutions, which employ hundreds of filters to detect all possible concepts of image content. Inspired by this, we introduce Pattern Embedding to convert the image $x \in R^{H \times W \times 3}$ into a compact sequence of visual words $x_{pattern} \in R^{N_{pattern} \times ((H', W') \cdot 1)}$, where (H', W') represents the resolution of each pattern, “1” represents a certain channel, $N_{pattern}$ is the resulting number of patterns. The pattern with $H' \times W' \times 1$ is detected by a specific filter, representing an independent semantic concept. And due to its global receptive field $H \times W$, each pattern does not disrupt the structural and semantic information. Furthermore, The sequence length $N_{pattern}$ is a hyperparameter ($N_{pattern} < N_{patch}$), which is smaller than the number of patches to ensure compact and efficient information. To achieve this, we design a heavy and flexible Tokenizer to meet all above.

Heavy Tokenizer We utilize the entire ResNet as a heavy Tokenizer to detect all potential image content concepts, for instance, patterns which are represented as each chan-

nel of output feature maps. Different from existing works, we view the entire pattern with a global receptive field as visual words, which is further fed to Transformer for global context learning.

Building Block and Width. BasicBlock (Basic) employs a stack of two 3x3 convolutions with a fixed width of 64. Bottleneck (Bottle) employs a stack of three convolutions with an optional width, where 1x1 layers adjust dimensions and the 3x3 layer acts as a reduced-dimension bottleneck. We utilize the Bottleneck with an optional width to balance speed and accuracy.

Changing stage ratio. The original design of the computation distribution across stages that makes ResNet more efficient than VGGNet is to apply strong resolution reductions with a relatively small computation budget in its first two stages. We further optimize the architecture for similar reasons and adjust the number of blocks in each stage from [3,4,6,3] in ResNet50 to [1,1,6,3]. Unlike existing designs, e.g., the stage ratio 1:1:9:1 in Swin Transformer, a heavy “stage4” greatly helps in extracting rich patterns.

Flexible Tokenizer The vanilla ViT (Dosovitskiy et al. 2020) has experimented with a hybrid vision transformer by stacking the Transformer above ResNet, and the patch embedding is applied to patches extracted from ResNet activation maps as illustrated in Figure 3a. The output activation map by ResNet is $x_1 \in C_1 \times H' \times W'$, where $H' = H/P, W' = W/P$, P is the downsampling size of ResNet.

$$x_2 = \text{Transpose}(\text{Flatten}(\text{Conv}(x_1))) \quad (1)$$

The input feature map of ViT is $x_2 \in N_{patch} \times C_2, N_{patch} = (H' \times W')$, where the length of patch sequence is constrained by H' and W' .

Removing Transpose Operation Traditional Transformers utilize self-attention to capture long-range dependencies among patches, thereby necessitating a Transpose operation to align the N_{patch} with the sequence length in Transformer during the Grafting process from ResNet to ViT. In contrast, our Pattern Transformer exactly removes the Transpose operation to align channels with the sequence length in Transformer, resulting in the computation of self-attention among patterns.

Model	Resnet			Transformer					Params	GFLOPs
	Block	Width	Stages	Tokens*	Embedding	Depth	Heads	Mlp ratio		
Res34 - ViTS	basic	64	[3,4,6,3]	128	384	12	6	4	42.8M	6.6
Res34 - ViTB	basic	64	[3,4,6,3]	128	768	12	12	4	106.6M	15.0
Res50 - ViTS	bottle	64	[3,4,6,3]	128	384	12	6	4	45.2M	7.0
Res50 - ViTB	bottle	64	[3,4,6,3]	128	768	12	12	4	109.0M	15.4
Efficient- <i>T</i>	bottle	32	[1,1,6,3]	64	192	6	6	2	11.9M	1.6
Efficient- <i>S</i>	bottle	64	[1,1,6,3]	64	384	6	6	2	29.8M	3.5
Efficient- <i>B</i>	bottle	96	[1,1,6,3]	64	576	6	6	2	56.7M	6.3

Table 1: Variants of our Pattern Transformer architecture. Tokens number represents the length of pattern sequence in Transformer

Introducing Extra Linear Transformation Pattern Transformer computes long-range dependencies among patterns, with each pattern $H' \times W' \times 1$ encompassing a global receptive field $H \times W$. As depicted in Figure 3b, we utilize a convolution to convert C_1 to N_{patch} for flexible adjustment of the pattern sequence length. Similarly, we introduce an extra Linear layer to convert $H' \times W'$ to C_2 for flexible adjustment of the dimension of patterns.

$$x_2 = \text{Linear}(\text{Flatten}(\text{Conv}(x_1))) \quad (2)$$

Consequently, this Grafting process facilitates the combination between any ResNet and ViT models, without consideration of their inherent feature size.

As a byproduct, we also introduce an extra Linear layer into the vanilla ViT, thereby constructing a flexible Patch Transformer as shown in Figure 3c.

$$x_2 = \text{Transpose}(\text{Linear}(\text{Flatten}(\text{Conv}(x_1)))) \quad (3)$$

For instance, the R50+ViT-B architecture in ViT (Dosovitskiy et al. 2020), constrained by the upstream ResNet output features size, used only 49 patches for the subsequent Transformer. Employing our Patch Transformer, we convert 49 patches up to 128 patches, significantly enhancing network performance.

Light Transformer

The Transformer layer consists of two alternating sub-layers of multi-head self-attention (MSA) and MLP blocks. Residual connections are applied around each sub-layer, followed by a layer normalization (LN). To facilitate residual connections, all sub-layers produce outputs with the same feature dimension. Given that heavy Resnet can extract high-level semantic patterns, we employ a relatively light Transformer to model global dependencies.

Reducing Transformer Tokens Token number in the vanilla ViT is determined by the image resolution and patch size, for instance, the length of the patch sequence is 196 in the ViT-B architecture. However, we utilize Pattern Transformer with an optional width, such as 64, to balance between speed and accuracy.

Reducing Depths and Heads The standard ViT contains 12 Transformer layers, with 12 parallel self-attention operations, called “heads”, in each layer. To reduce the computational cost, we utilize 6 Transformer layers with 6 heads.

Reducing the MLP block ratio The MLP block is a linear layer that increases the embedding dimension by a factor 4, applies a GELU non-linearity, and reduces it back with another linear layer to the original embedding’s dimension. To reduce the computational cost again, we decrease the expansion factor of the linear layer from 4 to 2.

Pattern Transformer Family

Pattern Transformer models can spawn a range of speed-accuracy trade-offs by altering the feature size in ResNet and ViT. Table 1 provides an overview of the models considered in our paper. For example, except for employing fewer tokens for the delicate Grafting, the parameters of Res34-ViTB adopt identical parameters as ResNet34 and ViT-B.

4 Experiments

We conduct comprehensive experiments to evaluate the effectiveness of our Pattern Transformer, including extensive ablative studies and visualization.

Datasets. Both large-scale ImageNet dataset and small-scale CIFAR dataset are adopted to evaluate our model. ImageNet dataset consists of 1.28M training images and 50k validation images from 1000 classes. CIFAR-10 and CIFAR-100 datasets consist of 50k training images and 10k validation images, respectively from 10 and 100 classes. Especially, all experiments on CIFAR datasets are trained from scratch.

Setting Up. We construct our Pattern Transformer by integrating the fundamental configurations of ResNet and ViT architectures. We primarily draw upon the training recipes in MAE (He et al. 2022) for stable training. Notably, we opt not to employ color jittering, repeated augmentation, gradient clipping, and layer scaling techniques. Moreover, we distinctly remove the strategies of random erasing and exponential moving average (EMA) in MAE. To capitalize on limited GPU resources, we leverage multiple gradient accumulation steps, enabling the effective large batch size. Specifically, for the CIFAR dataset, we employ a batch size of 1024 with 8 gradient accumulation iterations on a single NVIDIA GeForce RTX 3090 GPU. For the ImageNet dataset, we utilize a batch size of 4096 with 2 gradient accumulation iterations on four NVIDIA A100 GPUs. Furthermore, we report the final accuracy for 800 and 300 epochs on CIFAR and ImageNet datasets, respectively. And all other experiments on CIFAR datasets are conducted with

Method	Arch.	Params	GFLOPs	CIFAR-10	CIFAR-100
ResNet18 (Choi, Choi, and Kim 2022)	CNN	11.2M	-	90.27	63.41
ResNet50 (Choi, Choi, and Kim 2022)		23.5M	-	90.60	61.68
WRN28-10 (Zagoruyko and Komodakis 2016)		36.5M	5.2	96.00	80.75
ResNeXt-29, 8x64d (Xie et al. 2017)		34.4M	5.4	96.35	82.23
SENet-29 (Hu, Shen, and Sun 2018)		35.0M	5.4	96.32	82.22
SKNet-29 (Li et al. 2019)		27.7M	4.2	96.53	82.67
DeiT-S (Touvron et al. 2021)	Transformer	22.1M	4.3	92.44	69.78
DeiT-B (Touvron et al. 2021)		86.6M	16.9	92.41	70.49
PVT-S (Wang et al. 2021)		24.5M	3.8	92.34	69.79
Swin-S (Liu et al. 2021)		50.0M	-	94.17	77.01
Swin-B (Liu et al. 2021)		88.0M	-	94.55	78.45
CCT-7/3x1 (Hassani et al. 2021)	Transformer	3.8M	1.2	97.48	82.72
CCT-7/3x1 + TokenMixup (Choi, Choi, and Kim 2022)		3.8M	1.0	97.75	83.57
NesT-S (Zhang et al. 2022)		23.4M	6.6	96.97	81.70
NesT-B (Zhang et al. 2022)		90.1M	26.5	97.20	82.56
Patternformer (Res34-ViT _S)	Transformer	42.8M	6.6	97.72	83.27
Patternformer (Res34-ViT _B)		106.6M	15.0	97.78	84.29
Patternformer (Res50-ViT _S)		45.2M	7.0	97.73	82.95
Patternformer (Res50-ViT _B)		109.0M	15.4	97.68	84.96
Patternformer (Efficient-T)		11.9M	1.6	97.15	81.63
Patternformer (Efficient-S)		29.8M	3.5	97.61	82.33
Patternformer (Efficient-B)		56.7M	6.3	97.57	83.35

Table 2: Comparisons with previous results on CIFAR.

Method	Params	GFLOPs	ImageNet
DeiT-Ti (Touvron et al. 2021)	5.7M	1.1	72.2
ConViT-Ti (d’Ascoli et al. 2021)	6.0M	1.0	73.1
LocalViT-Ti (Li et al. 2021)	5.9M	1.3	74.8
PVT-Ti (Wang et al. 2021)	13.2M	1.9	75.1
Patternformer (Efficient-T)	11.9M	1.6	75.4

Table 3: Comparisons with previous results on ImageNet.

400 epochs. More comprehensive details are provided in the supplementary materials.

Comparison with Previous Works

As shown in Table 2, our Pattern Transformer achieves state-of-the-art performance on CIFAR-10 and CIFAR-100 datasets. On CIFAR-100 dataset, Pattern Transformer (Res50-ViT_B) attains the best performance with an accuracy of 84.96%, significantly surpassing the previous best model, CCT-7/3x1 + TokenMixup, which scored 83.57%. Additionally, Pattern Transformer (Res34-ViT_B) achieves a leading accuracy on CIFAR-10 at 97.78%, surpassing the existing benchmarks such as NesT-B (97.20%) and Token-Mixup (97.75%).

It’s worth noting that both CCT and NesT employ the network structures specifically designed for small datasets, especially CCT, which takes low-resolution images of 32×32 as inputs, significantly enhances computational efficiency. Setting aside these works, Pattern Transformer (Efficient-T) model, despite having only 11.9M parameters and requiring 1.6 GFLOPs, still achieved competitive performance with

97.15% accuracy on CIFAR-10 and 81.63% on CIFAR-100. This highlights the efficiency and effectiveness of our proposed method.

Table 3 gives the results of our proposed Pattern Transformer with several previous works on the ImageNet dataset. The Efficient-T variant of Pattern Transformer, with 11.9M parameters and 1.6 GFLOPs, achieves the best performance among the compared models with similar complexity. It outperforms DeiT-Ti, ConViT-Ti, LocalViT-Ti, and PVT-Ti by 3.2%, 2.3%, 0.6%, and 0.3% respectively. Notably, it achieves this superior performance with fewer parameters and computational complexity than PVT-Ti.

Ablation Study

We conduct in-depth ablation studies on numerous variants of the proposed Pattern Transformer, aiming at analyzing the influence of different architectural choices on the model performance. Our goal is to identify the key factors that contribute to improved accuracy, while concurrently considering the corresponding model parameters and computational complexity. We observed that an efficient Pattern

Block	Width	Params	GFLOPs	Acc(%)	Stages	Params	GFLOPs	Acc(%)	Stages	Params	GFLOPs	Acc(%)
bottle	8	90M	12.0	77.4	[0,0,0,0]	88M	11.7	63.6	[1,4,6,3]	106M	14.5	82.5
bottle	16	91M	12.3	79.0	[2,0,0,0]	88M	12.2	73.2	[3,1,6,3]	106M	14.3	82.5
bottle	32	96M	13.1	81.4	[2,2,0,0]	87M	12.4	77.2	[3,4,1,3]	101M	13.8	82.0
basic	64	107M	15.0	82.5	[2,2,2,0]	88M	12.7	80.3	[3,4,6,1]	97M	14.5	82.0
bottle	64	109M	15.4	82.7	[2,2,2,2]	97M	13.1	81.4	[1,1,6,3]	106M	13.8	82.2
bottle	96	129M	18.6	82.9	[3,4,6,3]	107M	15.0	82.5	[3,4,6,3]	107M	15.0	82.5

(a) Building block and width

(b) Depth

(c) Stage

Table 4: The impact of ResNet variations in building blocks, width, depth, and stages.

Tokens	Params	GFLOPs	Acc(%)	Embedding	Params	GFLOPs	Acc(%)	Depth	Params	GFLOPs	Acc(%)
8	107M	4.4	82.1	192	27M	4.4	82.6	3	43M	6.5	82.4
16	107M	5.1	82.4	384	43M	6.6	82.7	6	64M	9.3	82.6
32	107M	6.5	82.6	576	69M	10.0	83.0	9	85M	12.1	82.9
64	107M	9.3	82.7	768	107M	15.0	82.5	12	107M	15.0	82.5
128	107M	15.0	82.5	960	154M	21.2	82.4				

(a) Tokens

(b) Embedding

(c) Depth

Heads	Params	GFLOPs	Acc(%)
1	107M	15.0	82.4
3	107M	15.0	83.1
6	107M	15.0	83.0
8	107M	15.0	82.5
12	107M	15.0	82.5

(d) Heads

Mlp ratio	Params	GFLOPs	Acc(%)
1	64M	9.5	82.5
2	78M	11.3	83.1
3	92M	13.1	83.0
4	107M	15.0	82.5

(e) Mlp ratio

Table 5: The impact of Transformer variations in token number, embedding dimension, depth, attention heads, and MLP ratio.

Transformer relies on a combination of Heavy ResNet and Light Transformer. We set the Res34-ViT-B architecture in Table 1 as the baseline, distinctly denoted by a grey block, to facilitate better comparison.

Heavy ResNet ResNet captures all potential patterns within image content and we analyze the impact of ResNet variations in building blocks, width, depth, and different stages as discussed in Section 3. As illustrated in Table 4, we found that the model’s accuracy incrementally improves as the width of the building block expands. However, the increase in accuracy is accompanied by a growth in both model parameters and computational complexity. Similar to width, a deeper network, such as the stage architecture [3,4,6,3], enhances accuracy by capturing more complex patterns. We also explored the imports of different stage configurations. While reducing the building blocks in the first two stages maintained the original accuracy, reductions in the final two stages resulted in accuracy losses. This suggests that the latter stages play a more significant role in feature extraction. Overall, our ablation study indicates that the choice of building block, its width, the model’s depth, and stage configuration are all crucial to performance. Continual enhancement of these factors leads to consistent accuracy improvement, and we did not observe a saturation trend. However, this significantly escalates model parameters and computational complexity. A configuration using the “bottle” block with a width of 96 and a stage structure of [1,1,6,3] provides a good balance between accuracy, model

complexity, and computational costs.

Light Transformer Transformer models long-range dependencies among patterns and we examine various aspects of Transformer variations in token number, embedding dimension, network depth, attention heads, and MLP ratio as discussed in Section 3. The results are presented in Table 5. We observe a general trend of increasing accuracy with an increase in tokens, with the highest accuracy of 82.7% attained at 64 tokens. However, beyond this point, the accuracy decreases slightly, suggesting that there is an optimal token size for this task, after which the model performance may degrade due to overfitting or increased complexity. Similar to token number, embedding dimension, network depth, attention heads, and MLP ratio all play crucial roles in the model’s performance. The setting of 64 pattern tokens with an embedding dimension of 576 in a 6 layers of Transformer with 6 heads, 2 MLP ratio offers a good balance between accuracy, model complexity, and computational costs.

Discussions

Why does Pattern Transformer require a more complex tokenizer?

In conventional Vision Transformers, the size of the patches plays a pivotal role in balancing the speed-accuracy tradeoff, with smaller patches leading to higher accuracy but at a higher computational cost. For instance, the recent FlexiViT has found that ViT-B with a patch size of 8×8 achieves an accuracy of 85.6% on ImageNet1k with 156 GFLOPs,

Method	Tokenizer Layer	CIFAR100
Our Pattern Transformer		
ViT stem	1	54.9
Basic [0,0,0,0]	2	63.6
Basic [2,0,0,0]	6	73.2
Basic [3,4,6,3]	34	82.9
Bottle [3,4,6,3]	50	83.4
Bottle [3,4,6,4]	53	83.6
Our Patch Transformer		
Bottle [3,4,6,3]	50	83.7

Table 6: In-depth experiments of Network Depth.

whereas ViT-B with a patch size of 32×32 only attains an accuracy of 79.1% with 8.6 GFLOPs. This is due to the fact that as the patch size increases, the transformer struggles to optimize local information and is forced to reduce the sequence length. However, this also underscores the effectiveness of our Pattern Transformer in a way, as it can be simply seen as having a patch size of 224×224 , although it’s not entirely equivalent.

The Pattern Transformer maximizes the patch size, thus exacerbating the negative impacts mentioned above. As depicted in the figure 6, Pattern Transformer with one-layer tokenizer (similar to ViT stem) merely achieves an accuracy of 54.9%. To counter this, we necessitate a more complex tokenizer to extract higher-level semantic information. The Pattern Transformer with a 50-layer ResNet50 tokenizer can achieve an accuracy of 83.4%. By further increasing the fourth stage of the bottleneck block, an accuracy of 83.6% can be achieved. Therefore, this complexity is integral to the Pattern Transformer’s ability to excel in image classification tasks.

As a byproduct, our Flexible Patch Transformer, before being fed into the transformer, completely scrambles the original patch sequence space through an extra linear transformation (brutally converting 49 patches into 128 patches). This process entirely loses the interpretability, yet it achieves the best performance with an accuracy of 83.7%.

What exactly is the manifestation of Visual Words?

As we emphasized earlier, each pattern captures its local region of interest, thereby preserving its intrinsic structural and semantic information. To illustrate this, we visualized the Pattern Transformer (Res50-ViT-B) architecture, demonstrating the visual tokens before they are fed into the transformer. The Res50-ViT-B architecture generates a total of 128 patterns. We observed that certain patterns, such as 1st, 17th, 35th, and 102nd, consistently capture the foreground information of the object, while certain patterns like 2nd, 14th, 44th, 123th consistently capture the background information. As depicted in Figure 4, the first two columns invariably output the feature maps of the first and second patterns, while the third and fourth columns are selected randomly. We noted that the first pattern always prioritizes capturing the foreground related to humans, such as the low response

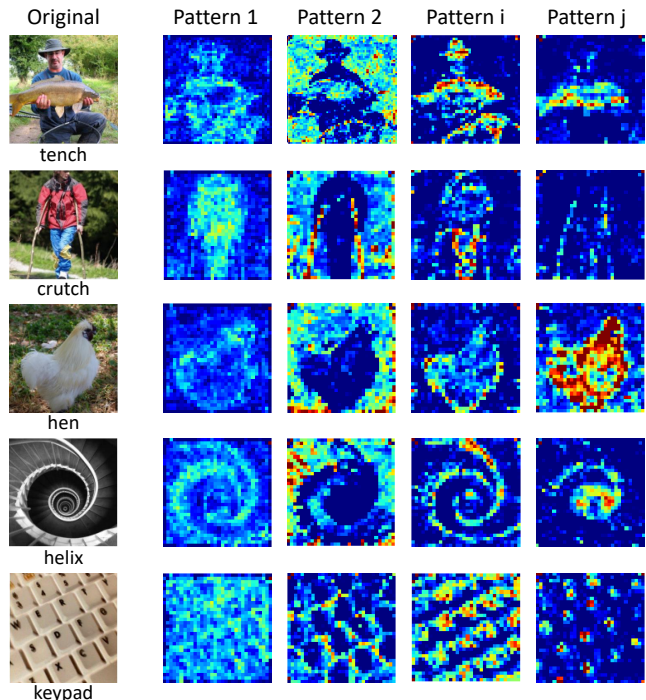


Figure 4: The visualization of Visual Words.

of fish overlapping with the human body in the “tench”. Conversely, the second pattern always prioritizes focusing on the interesting background, particularly the background interacting with humans, such as the cane in the “crutch”. Furthermore, for pattern j in the fourth column, we visualized interesting visual tokens, such as the fish in “tench” and the letters on “keypad”. These visualizations encompass comprehensive semantic information, further substantiating our claim, the efficacy of the Pattern Transformer in preserving the intrinsic structural and semantic information.

5 Conclusion

Pattern Transformer provides a novel solution to the challenge of converting images into sequence inputs for Vision Transformers. Traditional patchification disrupts the cohesion of structural and semantic details within images, constraining the potential of Transformer-based models. Pattern Transformer addresses these issues by dynamically converting images into pattern sequences. Leveraging Convolutional Neural Networks (CNNs), we extract localized patterns, assigning individual channels to specific patterns. These patterns are treated as visual words, seamlessly integrated into the Transformer network known for capturing global contextual relationships. By merging local patterns with global features, we effectively synergize CNNs and Transformers. Future work includes investigating the effectiveness of Pattern Transformer on other visual tasks such as detection and segmentation.

References

- Ali, A.; Touvron, H.; Caron, M.; Bojanowski, P.; Douze, M.; Joulin, A.; Laptev, I.; Neverova, N.; Synnaeve, G.; Verbeek, J.; et al. 2021. Xcit: Cross-covariance image transformers. *Advances in neural information processing systems*, 34: 20014–20027.
- Bau, D.; Zhou, B.; Khosla, A.; Oliva, A.; and Torralba, A. 2017. Network dissection: Quantifying interpretability of deep visual representations. In *Proceedings of the IEEE conference on computer vision and pattern recognition*, 6541–6549.
- Beyer, L.; Izmailov, P.; Kolesnikov, A.; Caron, M.; Kornblith, S.; Zhai, X.; Minderer, M.; Tschannen, M.; Alabdulmohsin, I.; and Pavetic, F. 2023. Flexivit: One model for all patch sizes. In *Proceedings of the IEEE/CVF Conference on Computer Vision and Pattern Recognition*, 14496–14506.
- Brown, T.; Mann, B.; Ryder, N.; Subbiah, M.; Kaplan, J. D.; Dhariwal, P.; Neelakantan, A.; Shyam, P.; Sastry, G.; Askell, A.; et al. 2020. Language models are few-shot learners. *Advances in neural information processing systems*, 33: 1877–1901.
- Chen, C.-F.; Panda, R.; and Fan, Q. 2021. Regionvit: Regional-to-local attention for vision transformers. *arXiv preprint arXiv:2106.02689*.
- Choi, H. K.; Choi, J.; and Kim, H. J. 2022. Tokenmixup: Efficient attention-guided token-level data augmentation for transformers. *Advances in Neural Information Processing Systems*, 35: 14224–14235.
- Devlin, J.; Chang, M.-W.; Lee, K.; and Toutanova, K. 2018. Bert: Pre-training of deep bidirectional transformers for language understanding. *arXiv preprint arXiv:1810.04805*.
- Dosovitskiy, A.; Beyer, L.; Kolesnikov, A.; Weissenborn, D.; Zhai, X.; Unterthiner, T.; Dehghani, M.; Minderer, M.; Heigold, G.; Gelly, S.; et al. 2020. An image is worth 16x16 words: Transformers for image recognition at scale. *arXiv preprint arXiv:2010.11929*.
- d’Ascoli, S.; Touvron, H.; Leavitt, M. L.; Morcos, A. S.; Biroli, G.; and Sagun, L. 2021. Convit: Improving vision transformers with soft convolutional inductive biases. In *International Conference on Machine Learning*, 2286–2296. PMLR.
- Graham, B.; El-Nouby, A.; Touvron, H.; Stock, P.; Joulin, A.; Jégou, H.; and Douze, M. 2021. Levit: a vision transformer in convnet’s clothing for faster inference. In *Proceedings of the IEEE/CVF international conference on computer vision*, 12259–12269.
- Guo, J.; Han, K.; Wu, H.; Tang, Y.; Chen, X.; Wang, Y.; and Xu, C. 2022. Cmt: Convolutional neural networks meet vision transformers. In *Proceedings of the IEEE/CVF Conference on Computer Vision and Pattern Recognition*, 12175–12185.
- Han, K.; Xiao, A.; Wu, E.; Guo, J.; Xu, C.; and Wang, Y. 2021. Transformer in transformer. *Advances in Neural Information Processing Systems*, 34: 15908–15919.
- Hassani, A.; Walton, S.; Shah, N.; Abuduweili, A.; Li, J.; and Shi, H. 2021. Escaping the big data paradigm with compact transformers. *arXiv preprint arXiv:2104.05704*.
- He, K.; Chen, X.; Xie, S.; Li, Y.; Dollár, P.; and Girshick, R. 2022. Masked autoencoders are scalable vision learners. In *Proceedings of the IEEE/CVF conference on computer vision and pattern recognition*, 16000–16009.
- He, K.; Zhang, X.; Ren, S.; and Sun, J. 2016. Deep residual learning for image recognition. In *Proceedings of the IEEE conference on computer vision and pattern recognition*, 770–778.
- Heo, B.; Yun, S.; Han, D.; Chun, S.; Choe, J.; and Oh, S. J. 2021. Rethinking spatial dimensions of vision transformers. In *Proceedings of the IEEE/CVF International Conference on Computer Vision*, 11936–11945.
- Howard, A. G.; Zhu, M.; Chen, B.; Kalenichenko, D.; Wang, W.; Weyand, T.; Andreetto, M.; and Adam, H. 2017. Mobilenets: Efficient convolutional neural networks for mobile vision applications. *arXiv preprint arXiv:1704.04861*.
- Hu, J.; Shen, L.; and Sun, G. 2018. Squeeze-and-excitation networks. In *Proceedings of the IEEE conference on computer vision and pattern recognition*, 7132–7141.
- Huang, G.; Liu, Z.; Van Der Maaten, L.; and Weinberger, K. Q. 2017. Densely connected convolutional networks. In *Proceedings of the IEEE conference on computer vision and pattern recognition*, 4700–4708.
- Huang, Z.; Ben, Y.; Luo, G.; Cheng, P.; Yu, G.; and Fu, B. 2021. Shuffle transformer: Rethinking spatial shuffle for vision transformer. *arXiv preprint arXiv:2106.03650*.
- Krizhevsky, A.; Sutskever, I.; and Hinton, G. E. 2012. Imagenet classification with deep convolutional neural networks. *Advances in neural information processing systems*, 25.
- Li, X.; Wang, W.; Hu, X.; and Yang, J. 2019. Selective kernel networks. In *Proceedings of the IEEE/CVF conference on computer vision and pattern recognition*, 510–519.
- Li, Y.; Zhang, K.; Cao, J.; Timofte, R.; and Van Gool, L. 2021. Localvit: Bringing locality to vision transformers. *arXiv preprint arXiv:2104.05707*.
- Liu, Z.; Lin, Y.; Cao, Y.; Hu, H.; Wei, Y.; Zhang, Z.; Lin, S.; and Guo, B. 2021. Swin transformer: Hierarchical vision transformer using shifted windows. In *Proceedings of the IEEE/CVF international conference on computer vision*, 10012–10022.
- Radosavovic, I.; Kosaraju, R. P.; Girshick, R.; He, K.; and Dollár, P. 2020. Designing network design spaces. In *Proceedings of the IEEE/CVF conference on computer vision and pattern recognition*, 10428–10436.
- Ryoo, M. S.; Piergiovanni, A.; Arnab, A.; Dehghani, M.; and Angelova, A. 2021. Tokenlearner: What can 8 learned tokens do for images and videos? *arXiv preprint arXiv:2106.11297*.
- Simonyan, K.; and Zisserman, A. 2014. Very deep convolutional networks for large-scale image recognition. *arXiv preprint arXiv:1409.1556*.
- Srinivas, A.; Lin, T.-Y.; Parmar, N.; Shlens, J.; Abbeel, P.; and Vaswani, A. 2021. Bottleneck transformers for visual recognition. In *Proceedings of the IEEE/CVF conference on computer vision and pattern recognition*, 16519–16529.

Su, X.; You, S.; Xie, J.; Zheng, M.; Wang, F.; Qian, C.; Zhang, C.; Wang, X.; and Xu, C. 2022. ViTAS: Vision transformer architecture search. In *European Conference on Computer Vision*, 139–157. Springer.

Szegedy, C.; Liu, W.; Jia, Y.; Sermanet, P.; Reed, S.; Anguelov, D.; Erhan, D.; Vanhoucke, V.; and Rabinovich, A. 2015. Going deeper with convolutions. In *Proceedings of the IEEE conference on computer vision and pattern recognition*, 1–9.

Tan, M.; and Le, Q. 2019. Efficientnet: Rethinking model scaling for convolutional neural networks. In *International conference on machine learning*, 6105–6114. PMLR.

Touvron, H.; Cord, M.; Douze, M.; Massa, F.; Sablayrolles, A.; and Jégou, H. 2021. Training data-efficient image transformers & distillation through attention. In *International conference on machine learning*, 10347–10357. PMLR.

Vaswani, A.; Shazeer, N.; Parmar, N.; Uszkoreit, J.; Jones, L.; Gomez, A. N.; Kaiser, Ł.; and Polosukhin, I. 2017. Attention is all you need. *Advances in neural information processing systems*, 30.

Wang, P.; Wang, X.; Wang, F.; Lin, M.; Chang, S.; Li, H.; and Jin, R. 2022. Kvt: k-nn attention for boosting vision transformers. In *European conference on computer vision*, 285–302. Springer.

Wang, W.; Xie, E.; Li, X.; Fan, D.-P.; Song, K.; Liang, D.; Lu, T.; Luo, P.; and Shao, L. 2021. Pyramid vision transformer: A versatile backbone for dense prediction without convolutions. In *Proceedings of the IEEE/CVF international conference on computer vision*, 568–578.

Wu, H.; Xiao, B.; Codella, N.; Liu, M.; Dai, X.; Yuan, L.; and Zhang, L. 2021. Cvt: Introducing convolutions to vision transformers. In *Proceedings of the IEEE/CVF international conference on computer vision*, 22–31.

Xie, S.; Girshick, R.; Dollár, P.; Tu, Z.; and He, K. 2017. Aggregated residual transformations for deep neural networks. In *Proceedings of the IEEE conference on computer vision and pattern recognition*, 1492–1500.

Yin, H.; Vahdat, A.; Alvarez, J. M.; Mallya, A.; Kautz, J.; and Molchanov, P. 2022. A-vit: Adaptive tokens for efficient vision transformer. In *Proceedings of the IEEE/CVF Conference on Computer Vision and Pattern Recognition*, 10809–10818.

Yuan, K.; Guo, S.; Liu, Z.; Zhou, A.; Yu, F.; and Wu, W. 2021. Incorporating convolution designs into visual transformers. In *Proceedings of the IEEE/CVF International Conference on Computer Vision*, 579–588.

Zagoruyko, S.; and Komodakis, N. 2016. Wide residual networks. *arXiv preprint arXiv:1605.07146*.

Zhang, Z.; Zhang, H.; Zhao, L.; Chen, T.; Arik, S. Ö.; and Pfister, T. 2022. Nested hierarchical transformer: Towards accurate, data-efficient and interpretable visual understanding. In *Proceedings of the AAAI Conference on Artificial Intelligence*, volume 36, 3417–3425.

Zhou, D.; Kang, B.; Jin, X.; Yang, L.; Lian, X.; Jiang, Z.; Hou, Q.; and Feng, J. 2021. Deepvit: Towards deeper vision transformer. *arXiv preprint arXiv:2103.11886*.

A More Discussions

Compact Visual Words

Images inherently possess a high level of redundancy. Manual partitioning of images into a fixed number of patches often produces redundant and uninformative patches for the target class. These redundant patches not only fail to provide beneficial information but also impose a computational burden on expensive Transformer. As exemplified in Figure 5,

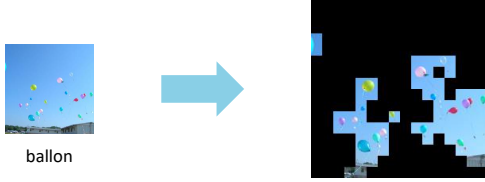


Figure 5: Vision Transformer contains redundant patches.

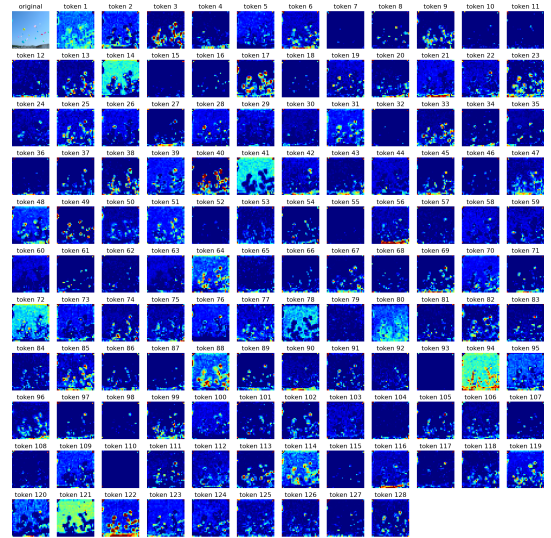
merely 68 out of 256 patches furnish discriminative information for the "balloon" class, whereas the remaining 188 patches predominantly contain superfluous details, such as sky, buildings, trees, etc. All these redundant patches partake in the subsequent Transformer computations, thereby exacerbating the redundancy. This amplification of redundancy becomes particularly pronounced when objects are situated at a considerable distance.

Pattern Transformer converts the image into a sequence of patterns (visual tokens), where each pattern captures the local region of interest. These patterns are autonomously optimized by the network, progressively extracting features. As depicted in Figures 6a and 6b, we have visualized 128 various patterns in Res50 - ViTB and 64 patterns in Efficient-*B* respectively. The majority of these patterns capture the balloon area, with varying responses focusing on different balloon aspects. A handful of these features exhibit low response activation or may concentrate on the background area, a phenomenon less frequent in Efficient architecture. Anyway, compared to the conventional Transformer, our Pattern Transformer is more compact and efficient.

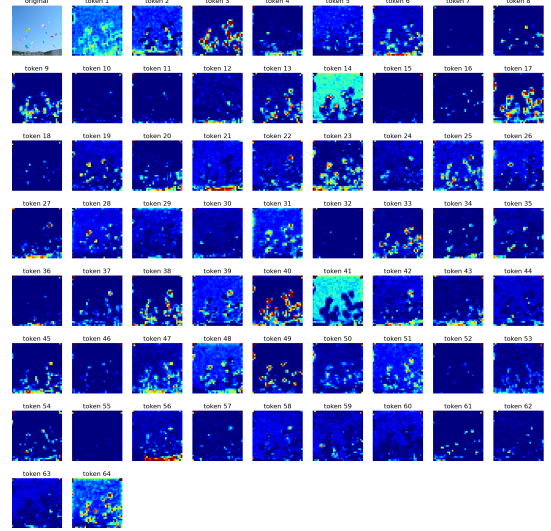
Semantic Consistency

Images, especially complex ones, often depict identical objects with different geometric variations caused by rotation and scale. Manually dividing these images into rigid patches based on experiential knowledge results in inconsistent semantic information. As exemplified in Figure 7, considerable changes occur in the patch sequence of the same image after simple cropping or rotation operations.

Convolutional neural networks excel at capturing intricate patterns, and our Pattern Transformers naturally inherit its ability to process shift-invariant patterns in images. Figure 8 visualizes patterns (visual tokens) under cropping, rotation, and cropping with rotation, observing consistent semantic information. For instance, token 1 invariably prioritizes capturing the foreground related to specific information, such as penguins. Conversely, token 2 consistently focuses on the interesting background, like coastlines. These observations



(a) 128 patterns in our Res50 - ViTB architecture.



(b) 64 patterns in our Efficient-*B* architecture.

Figure 6: The visualization of compact visual tokens.

indicate that our Pattern Transformer maintains excellent semantic consistency.

Preservation of Complete Structure

Traditional Transformers inherently depend on sequential input, necessitating the manual partitioning of images into patch sequences, which disrupts the inherent image structure. In contrast, Pattern Transformer converts the image into a sequence of patterns. Thanks to its global receptive field, it can capture all potential image content concepts, thereby preserving the complete structural information.

Flexible Sequence Length

The sequence length of the traditional Transformer is determined by the image resolution and patch size, which limits the model's potential and flexibility. Our Pattern Trans-

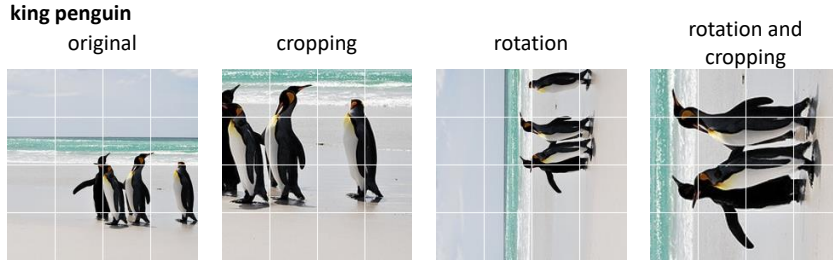


Figure 7: Semantic inconsistency in Vision Transformer.

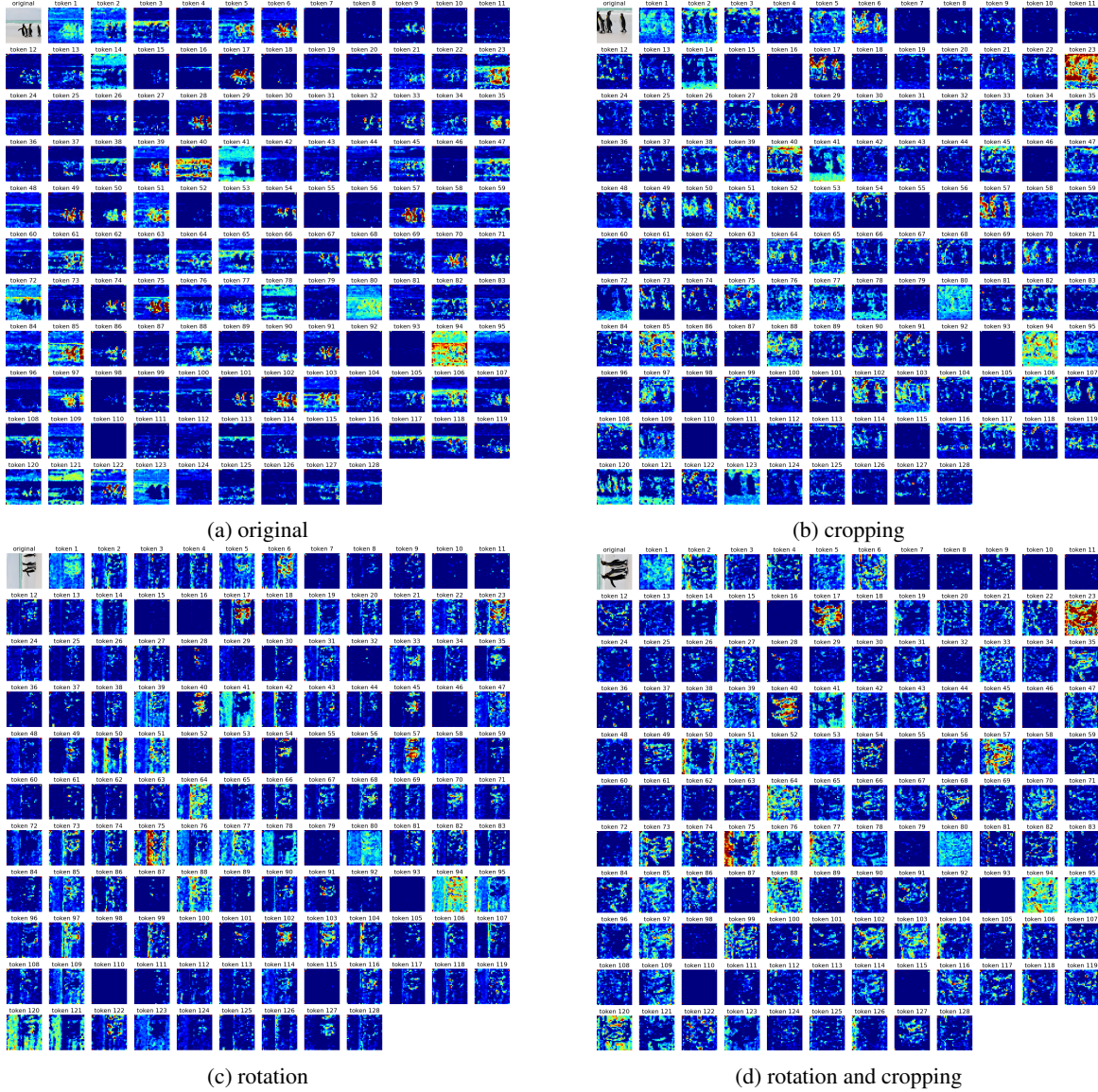


Figure 8: The visualization of semantically consistent visual tokens.

former aligns channels with the sequence length in Transformer, enabling the computation of self-attention among patterns of a flexible value, which provides a trade-off between speed and accuracy.

Limitations

Revisiting the experiment results outlined in Section 4, our Pattern Transformer (Res50-ViT-B) demonstrates the best performance, achieving an impressive accuracy of 84.96%, significantly outperforming prior works by a large margin. Notably, the Pattern Transformer (Efficient-T), despite its compact architecture with merely 11.9M parameters and requiring 1.6 GFLOPs, still delivers a competitive performance of 81.63%. However, we noticed generally low performance across pure transformers. For instance, Swin-B, despite boasting 88M parameters, only reaches an accuracy of 78.5%, while DeiT-B yields an even lower performance, with an accuracy of just 70.5%. These observations prompt us to delve deeper into the underlying causes of these phenomena.

As illustrated in Figure 7, we retrained the ViT-B and ResNet50 on CIFAR-100 under identical settings, yielding intriguing results. Specifically, our reimplementation ResNet50 achieved an accuracy of 81.9%. This sheds light on three key phenomena:

- The benefits derived from the convolutions play a pivotal role.
- By utilizing patterns from convolutional networks as visual tokens and further deploying transformers to model global information, we can capture more comprehensive features. Compared to ResNet50, the Pattern Transformer (Res50-ViT-B) still offers a performance improvement of 1.5
- The conventional convolution, when combined with novel training strategies, still maintains a significant advantage on CIFAR-100. We have identified and provided a superior training recipe for ResNet50.

Moreover, this further corroborates our assertion in Section 4 that the performance would markedly deteriorate when employing a lightweight tokenizer. This implies that the limitations of the Pattern Transformer lie in its need for robust and efficient pattern extraction.

Method	CIFAR100
ViT-B (Zhang et al. 2022)	70.5
ResNet50 (Choi, Choi, and Kim 2022)	61.7
ViT-B	75.2
ResNet50	81.9
Patternformer (Res50-ViT-B)	83.4

Table 7: Ablation Studies on two factions

More Visualization

We provide more visualization results at the end of our paper as shown in Figure 9 - 12. These results further substantiate the efficacy of our Pattern Transformer and visually offer a more comprehensive understanding of our research.

B Experiment Details

Further details on our experimental settings are provided in Table 8. In contrast to recent studies, which often differ in

regularization and augmentation usage, frequently intensify these with larger model sizes to prevent overfitting and enhance accuracy, our method maintains a consistent training recipe across all variants and delivers robust performance without extensive hyper-parameter search.

Config	Value
Resolution (Train and Test)	224 × 224
Optimizer	AdamW
Batch size	1024(C), 4096(I)
Base learning rate	2e-4(C), 1e-4(I)
Learning rate schedule	cosine
layer-wise lr decay	0.65
Weight decay	0.3
Momentum	$\beta_1, \beta_2 = 0.9, 0.95$
Training epochs	800(C), 300(I)
Warmup epochs	5(C), 20(I)
Label smoothing	0.1
Dropout	×
Drop path	0.1
Repeated Aug	×
Gradient Clip	×
Rand Augment	9 / 0.5
Mixup	0.8
Cutmix	1.0
Erasing prob	×
ColorJitter	×
PCA lighting	×
Loss	CE
LayerScale	×
SWA	×
EMA	×

Table 8: Training settings. “C” represents CIFAR-10 and CIFAR-100 datasets, while “I” represents ImageNet dataset.

Strategies	CIFAR100
Patternformer (Res50-ViT-B)	83.4
w.o. smooth	82.7
w.o. cutmix	81.3
w.o. mixup	82.3
w.o. drop path	83.3

Table 9: Ablation Studies on Training Methods

Notably, we adopt the linear lr scaling rule: $lr = \text{base } lr \times \text{batchsize} / 256$. Moreover, we employ global average pooling features for the final classification, rather than the class token. Further ablation experiments regarding the training strategies employed above on CIFAR-100 are detailed in Table 9. All cifar ablation experiments are conducted over 400 epochs.

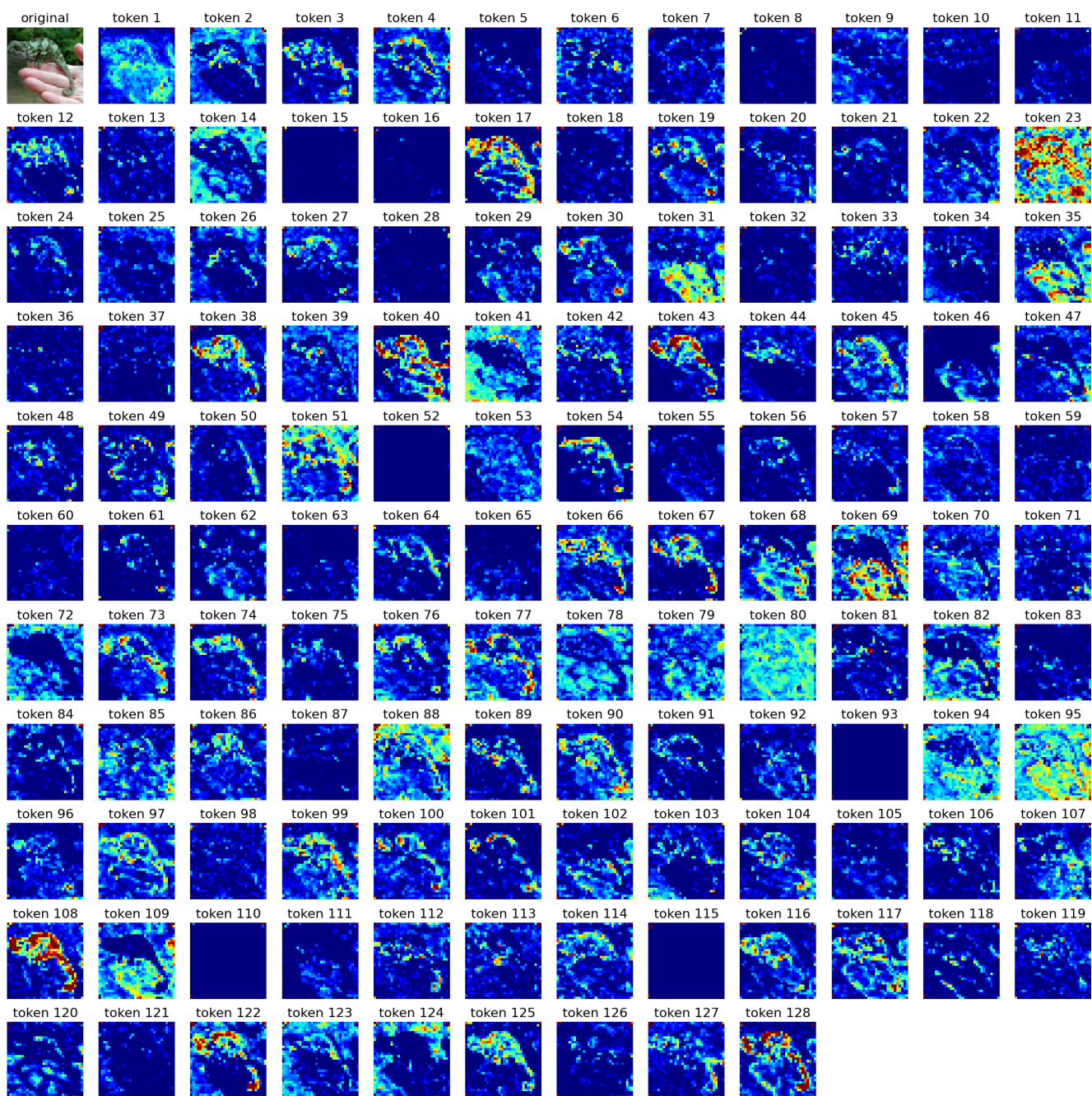


Figure 9: The visualization of visual tokens for “African chameleon”.

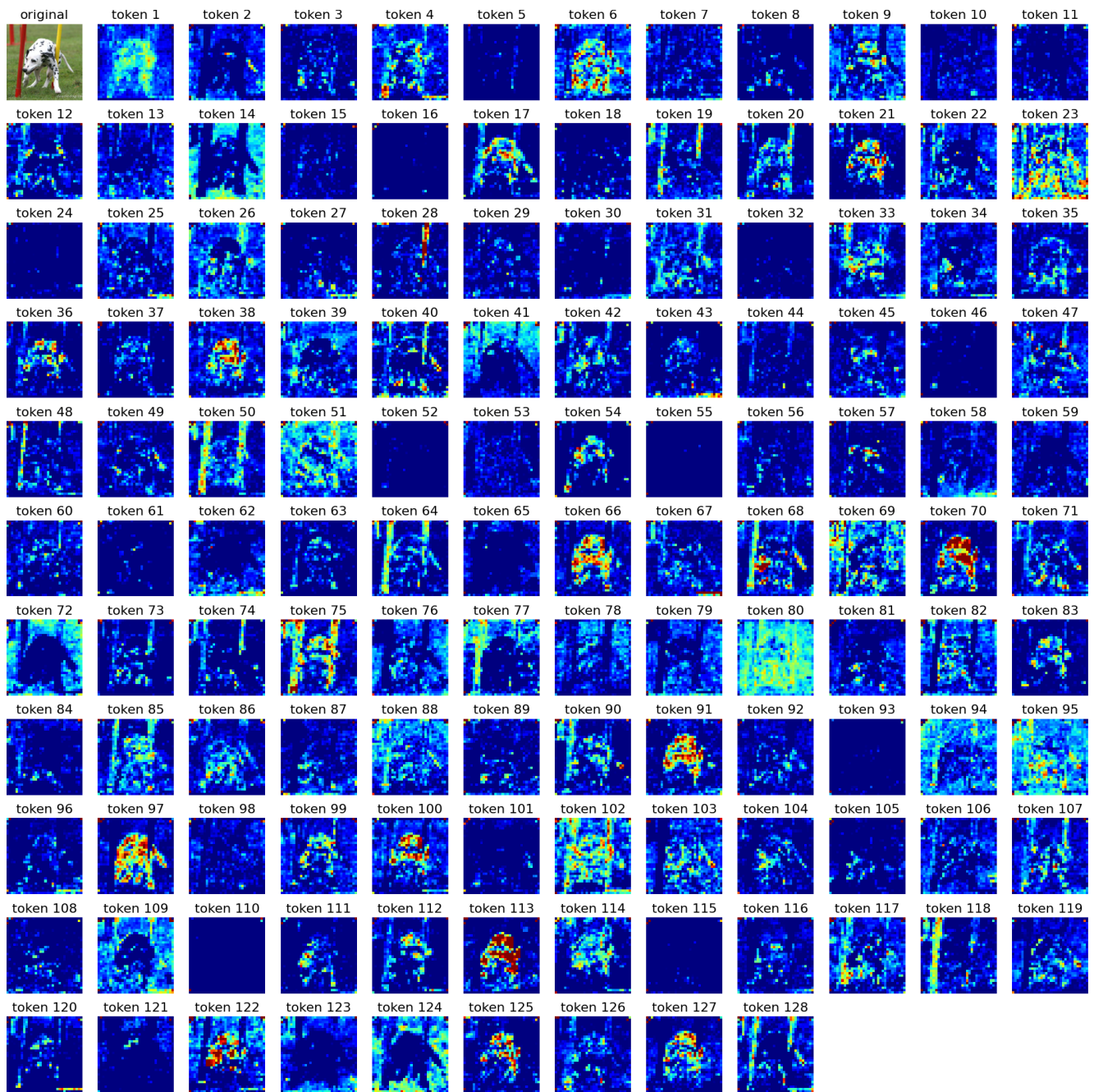


Figure 10: The visualization of visual tokens for “dalmatian”.

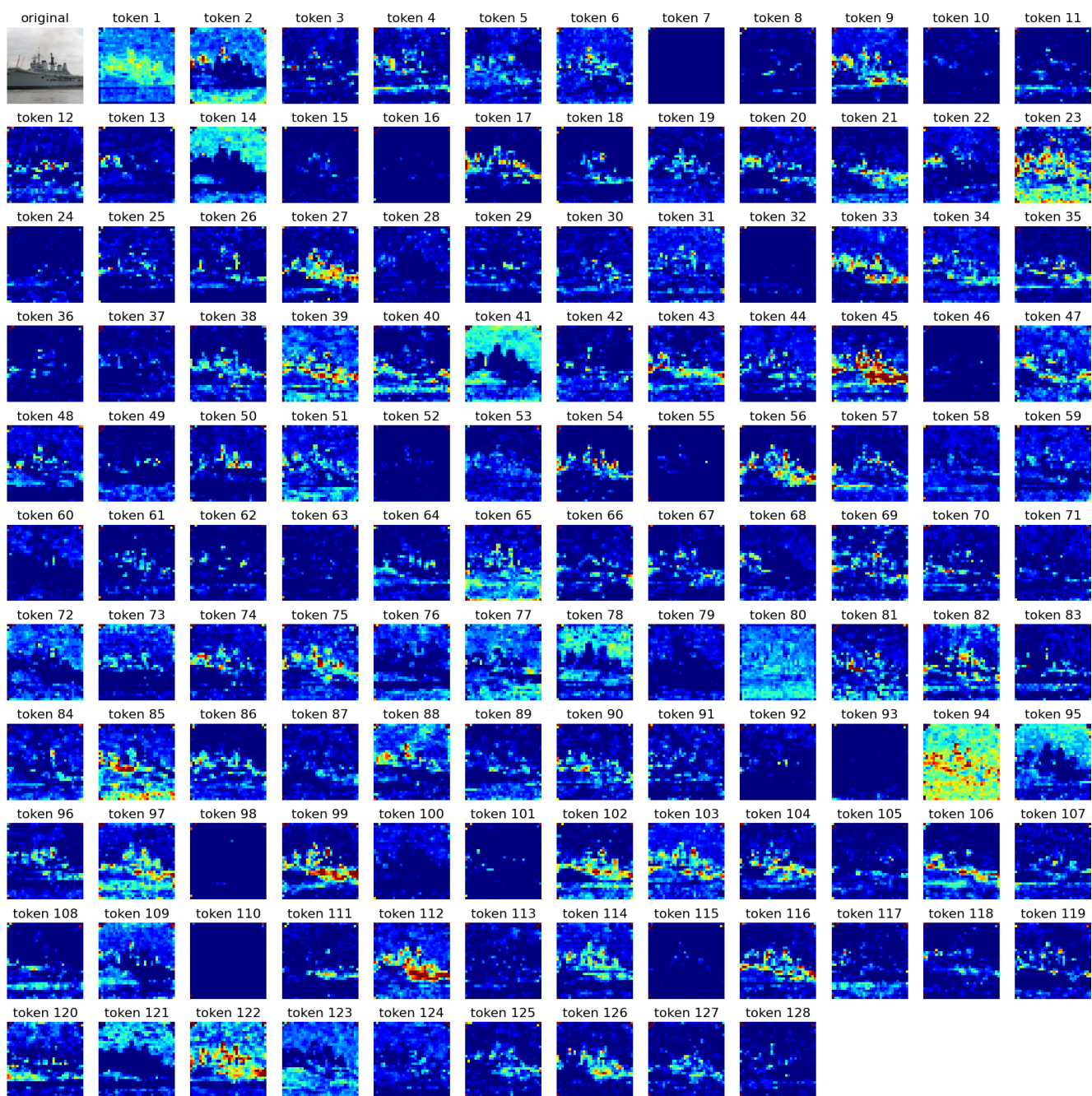


Figure 11: The visualization of visual tokens for “aircraft carrier”.

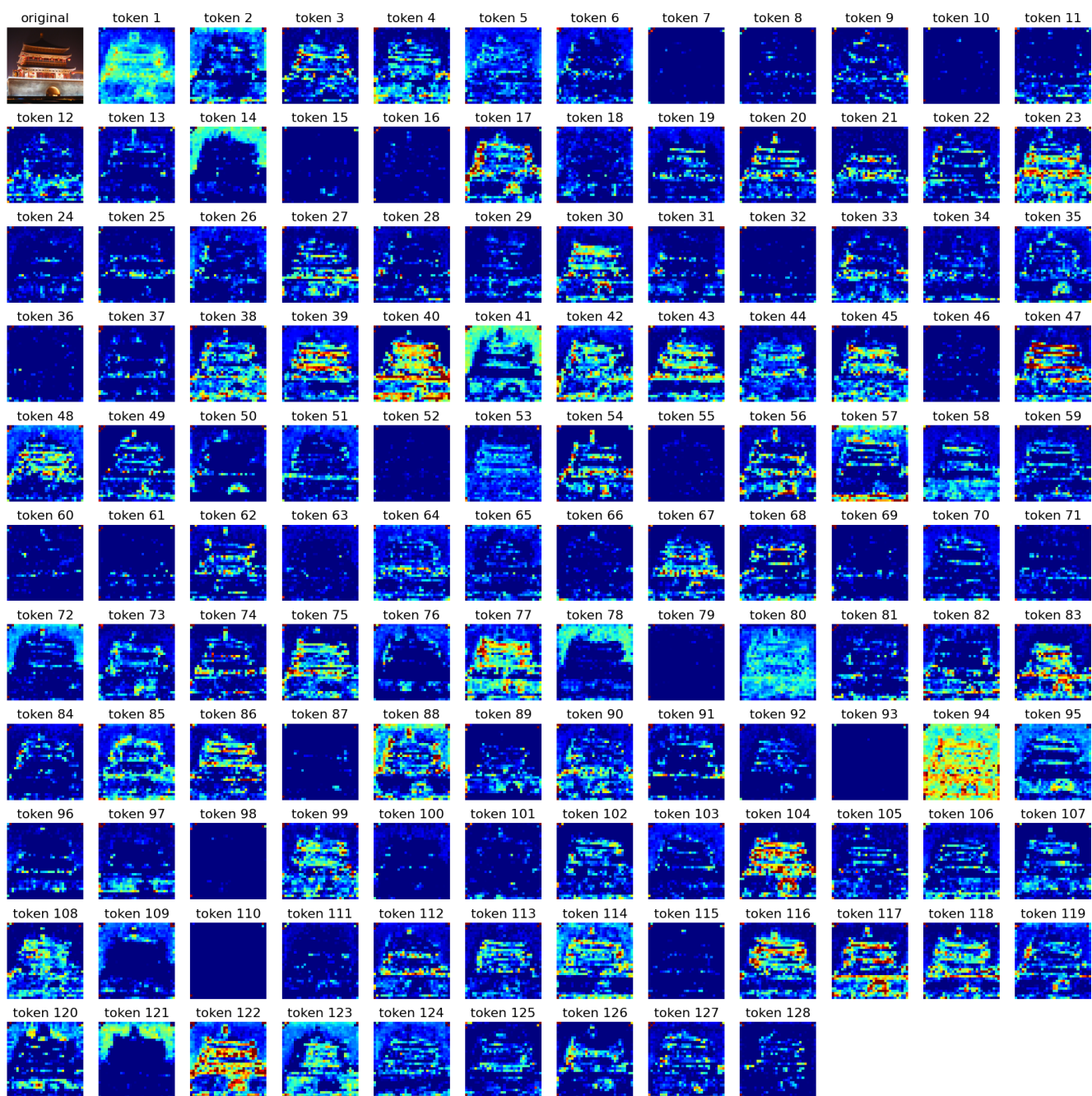


Figure 12: The visualization of visual tokens for “bell cote”.